

## Accepted version on Author's Personal Website: C. R. Koch

Article Name with DOI link to Final Published Version complete citation:

M. Aliramezani, C. R. Koch, and R. E. Hayes. Estimating tailpipe nox concentration using a dynamic nox/ammonia cross sensitivity model coupled to a three state control oriented scr model. In *IFAC Advances in Automotive Controls Conference (AAC), Sweden*, volume 49, pages 8–13. Elsevier, June 2016

### See also:

[https://sites.ualberta.ca/~ckoch/open\\_access/Aliramezani2016aac.pdf](https://sites.ualberta.ca/~ckoch/open_access/Aliramezani2016aac.pdf)

Post-print

As per publisher copyright is ©2016



This work is licensed under a  
[Creative Commons Attribution-NonCommercial-NoDerivatives 4.0 International License](https://creativecommons.org/licenses/by-nc-nd/4.0/).



Article accepted version starts on the next page →

[Or link: to Author's Website](#)

# Estimating tailpipe NO<sub>x</sub> concentration using a dynamic NO<sub>x</sub>/ammonia cross sensitivity model coupled to a three state control oriented SCR model

M. Aliramezani\* C.R. Koch\* R. E. Hayes\*\*

\* *Department of Mechanical Engineering, University of Alberta, Edmonton, AB T6G 2G8, Canada (e-mail: aliramez@ualberta.ca)*

\*\* *Department of Chemical and Materials Engineering, University of Alberta, Edmonton, AB T6G 2G8, Canada*

---

**Abstract:** A dynamic  $NO_x$  sensor model is developed to remove ammonia cross sensitivity from production  $NO_x$  sensors mounted downstream of Diesel-engine selective catalytic reduction (SCR) systems. The model is validated for large amounts of ammonia slip during different engine transients. A three-state nonlinear control oriented SCR model is also developed to predict the  $NH_3$  concentration downstream of the SCR ( $NH_3$  slip).  $NH_3$  slip is then used as an input for modeling the cross sensitivity of a production  $NO_x$  sensor and calculating the actual  $NO_x$  concentration in the presence of  $NH_3$  contamination. The cross sensitivity is considered to be a function of temperature, normalized ammonia slip rate (NASR) and time. The validation results show that the developed model has an acceptable accuracy for the actual  $NO_x$  concentration downstream of the SCR. This model should be of utility for engine emission control strategies such as SCR control.

*Keywords:* NO<sub>x</sub> sensor, Empirical sensor model, Cross-sensitivity factor, Dynamic model, SCR, Control-oriented modeling, Diesel engines, Emission control.

---

## 1. INTRODUCTION

The high efficiency and fuel economy advantages of Direct Injection (DI) Diesel engines make them interesting for power generation systems. However, new engine control strategies and after treatment systems are needed to meet stringent  $NO_x$  and particulate emission regulations.

Urea-based selective catalytic reduction (SCR) is an effective technique to reduce the  $NO_x$  emissions and to satisfy future emission standard regulations (Koebel et al., 2000; Zhang and Wang, 2015). Measuring the  $NO_x$  concentration in the exhaust gas is essential for closed-loop control of SCR systems (Devarakonda et al., 2008; Jones and Geveci, 2011; Frobert et al., 2013). However, the commercial  $NO_x$  sensors are cross-sensitive to ammonia ( $NH_3$ ). Due to this cross sensitivity, the  $NO_x$  sensor reading can defer from the actual value (Zhang et al., 2015). Determining actual  $NO_x$  is an important challenge for controlling urea injection of SCR systems.

Cross sensitivity of commercial  $NO_x$  sensors to  $NH_3$ , makes it difficult to achieve maximum  $NO_x$  conversion in SCR control. The time delay in the urea or ammonia injection and SCR catalyst dynamics are the other important factors that limit the performance of closed-loop SCR control (Willems et al., 2007).

The cross-sensitivity factor is taken as a constant by Hsieh and Wang (2010); Bonfils et al. (2014) and a function of time by Zhang et al. (2015) and the normalized stoichio-

metric ratio by Devarakonda et al. (2009). However, none of these studies capture all the cross sensitivity factors of commercial  $NO_x$  sensors and the models can still be improved.

In this work, available cross sensitivity models are first evaluated. Then, a temperature-based function is derived for the cross sensitivity factor based on experimented data. The model is then improved for transients by adding a correction factor. A new parameter (normalized ammonia slip rate) is defined which is an effective factor on cross sensitivity in transients. A three state model is calibrated, used to predict  $NH_3$  slip and the results are validated using experimental data.

Finally, the SCR model and the sensor model are coupled and  $NO_x$  concentration is estimated using the  $NO_x$  sensor signal decomposition. The validation results show that the model is capable of accurately estimating the actual  $NO_x$  concentration based on the  $NH_3$  and  $NO_x$  concentration upstream of the SCR and the  $NO_x$  sensor signal located downstream of the SCR for the data tested.

## 2. NO<sub>x</sub> SENSOR MODEL

A linear form of a NO<sub>x</sub> sensor model from Schar et al. (2006) is:

$$\overline{C_{NO_x}} = C_{NO_x} + C_{CS}C_{NH_3} \quad (1)$$

Where,  $\overline{C_{NO_x}}$  is the sensor output signal,  $C_{CS}$  is the cross sensitivity factor.  $C_{NO_x}$  and  $C_{NH_3}$  are  $NO_x$  and

$NH_3$  concentrations respectively. Rearranging Eqn. (1), the actual  $NO_x$  concentration is:

$$C_{NO_x} = \overline{C_{NO_x}} - C_{CS}C_{NH_3} \quad (2)$$

The cross-sensitivity factor is taken to be: a constant (Hsieh and Wang, 2010; Bonfils et al., 2014); a function of time (Zhang et al., 2015) and the normalized stoichiometric ratio (Devarakonda et al., 2009). However, commercial sensors are complex and as shown, these models can be improved for transient conditions or when there is large amounts of  $NH_3$  slip. In the next section, experimental data in the literature (Hsieh and Wang, 2011) is used to evaluate different cross sensitivity models. Two tests are chosen from the experimental data and are described in Table 1, with details in Hsieh and Wang (2011).

Test number	Test 1	Test 2
Engine speed range (rpm)	1700	1000
Engine torque range (Nm)	265-285	235-250
Gas Temperature before SCR (C)	270-333	245-250
AdBlue Inj. Rate (mg/sec)	145	107

Table 1. Tests description (Hsieh and Wang, 2011)

The measured values from Horiba MEXA 7500 gas analyzer after the SCR and  $NO_x$  concentration estimates for different constant cross sensitivity factors are shown in Fig. 1 and 2, where  $C_{NO_x}$ ,  $C_{NH_3}$  are measured from downstream of the SCR and the temperature is for exhaust gas upstream of the SCR. Both tests have transient Adblue injection (Hsieh and Wang, 2011).

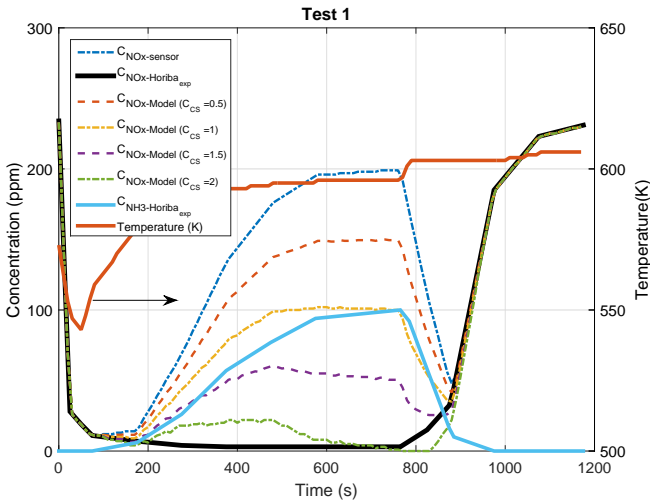


Fig. 1. Modeled  $NO_x$  concentration for constant cross sensitivity factors vs. actual concentration - test 1 (Hsieh and Wang, 2011)

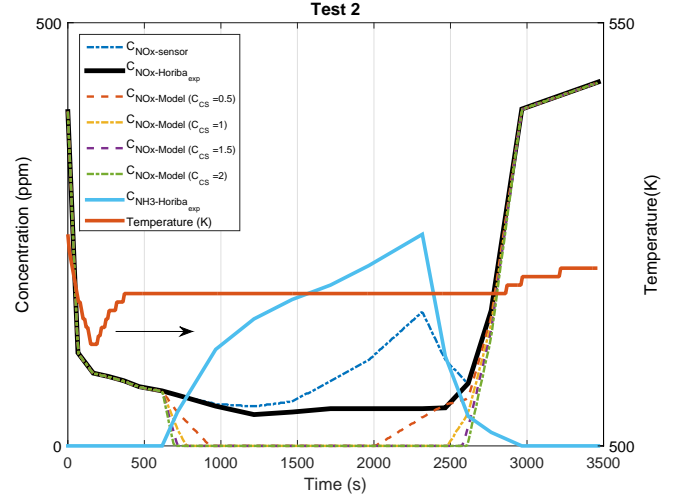


Fig. 2. Modeled  $NO_x$  concentration for constant cross sensitivity factors vs. actual concentration - test 2 (Hsieh and Wang, 2011)

The actual  $NO_x$  concentration is taken as the measured value from Horiba gas analyser (the solid black line). The output signal from the production  $NO_x$  sensor (the dot-dashed blue line) shows a significant deviation from the actual  $NO_x$  concentration. Since the Horiba gas analyser also measures  $NH_3$ , different cross-sensitivity factors are checked using the ammonia slip and the  $NO_x$  sensor reading as shown in Fig. 1 and 2 for tests 1 and 2 respectively. The use of a constant cross sensitivity of 0.5, 1, 1.5 and 2 in Eqn. (2) are also shown as the four dashed lines. Even with constant cross sensitivity, the  $NO_x$  sensor model error is significant. This error is attributed to exhaust gas temperature deviation between the tests.

The cross sensitivity factor is found varying with exhaust gas temperature over a bounded range (Hsieh and Wang, 2011; Zhang et al., 2015). The function  $\arctan(T)$  is used as a simple function dependence of temperature (T). To achieve this

$$\overline{C_{CS}(T)} = a * \arctan((T - b) * c) + d \quad (3)$$

is used for cross sensitivity as a function of temperature with T[K] and  $a$ ,  $b$ ,  $c$  and  $d$  are parameters which are fit to the experimented data from Hsieh and Wang (2011) and listed in Table 2.

Parameter	Value
a	0.65
b	550
c	0.1
d	1.087

Table 2. Calibrated parameters in Eqn. (3)

The estimate of  $NO_x$  concentration for the two cases above including the temperature dependent cross sensitivity are shown in Fig. 3 and 4. Estimated NOx has a maximum error of 34 ppm and 48 ppm for tests 1 and 2 respectively using a **single** cross sensitivity function. This is significantly lower error than with constant cross sensitivity.

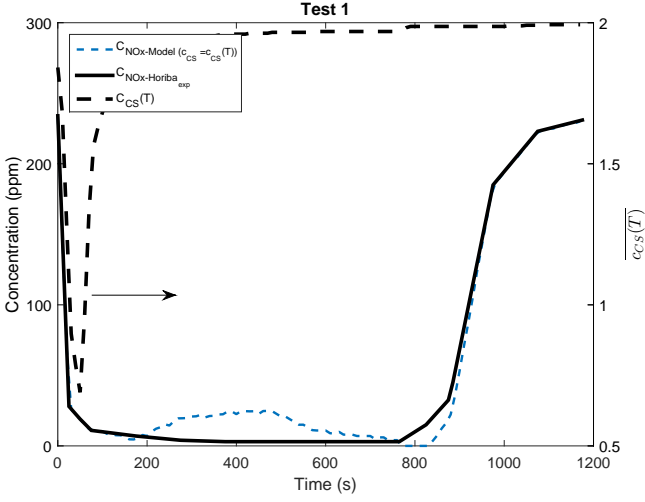


Fig. 3. Modeled  $NO_x$  concentration from the temperature-based cross sensitivity ( $\overline{c_{CS}(T)}$  - test1) - maximum error: 34 ppm

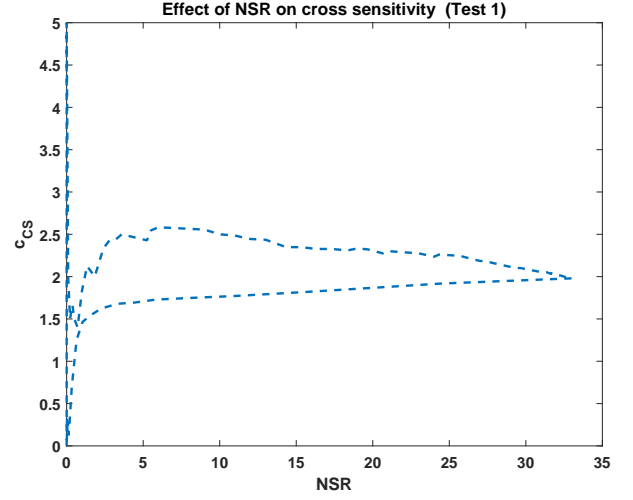


Fig. 5. Effect of NSR on cross sensitivity (test1)

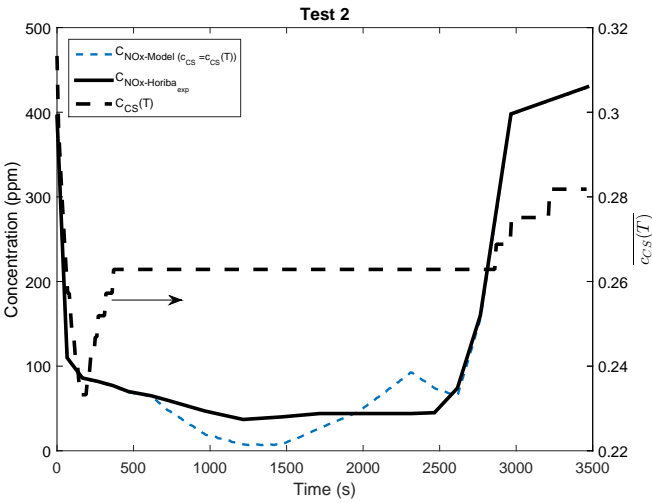


Fig. 4. Modeled  $NO_x$  concentration from the temperature-based cross sensitivity ( $\overline{c_{CS}(T)}$  - test2) - maximum error: 48 ppm

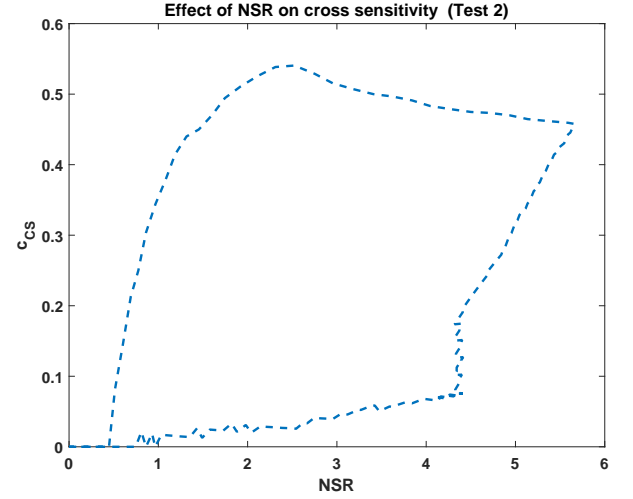


Fig. 6. Effect of NSR on cross sensitivity (test2)

To further improve the model transient response, normalized stoichiometric ratio (NSR) is used (Devarakonda et al., 2009). NSR is defined as the fraction of  $NH_3$  concentration over  $NO_x$  concentration:

$$NSR = \frac{C_{NH_3}}{C_{NO_x}} \quad (4)$$

However, as shown in Fig. 5 and 6, the relation between cross sensitivity and NSR is not static and changes with the time over the two tests.

To include time dependence, a new factor is proposed:

$$\beta = \frac{dC_{NH_3}}{dt} \cdot C_{NH_3} \quad (5)$$

In Eqn. (5),  $C_{NH_3}$  is the measured ammonia concentration from Horiba MEXA 7500 (Hsieh and Wang, 2011).

Then,  $\overline{c_{CS}(T)}$  in Eqn. (3) is augmented to include a transient correction factor,  $\overline{k(\beta)}$  as:

$$\overline{c_{CS}(T, \beta)} = \overline{k(\beta)} \overline{c_{CS}(T)} \quad (6)$$

Where,  $\overline{c_{CS}(T)}$  is calculated from Eqn. (3).

The calibrated values of  $\overline{k(\beta)}$  from the experimented data for different ranges of  $\beta$  is shown in Table 3.

The transient correction factor,  $\overline{k(\beta)}$ , adds step changes to the model when  $\beta$  changes sign. This is undesirable so a first order low pass filter is used with a time constant that is a function of temperature.

$\beta$	$\overline{k(\beta)}$
$> 0$	1.1
$= 0$	1
$< 0$	0.8

Table 3. Transient correction factor  $\overline{k(\beta)}$  in Eqn (6)

Considering  $\beta$  as a function of time, the first order low pass filter has the following form:

$$K(\beta(s), T) = \frac{1}{\tau(T)s + 1} \overline{K(\beta(s))} \quad (7)$$

Then:

$$k(\beta, T, t) = \mathcal{L}^{-1}\{K(\beta(s), T)\} \quad (8)$$

The result from Eqn. (6) has the form:

$$c_{CS}(\beta, T, t) = k(\beta, T, t) \overline{c_{CS}(T)} \quad (9)$$

with  $T$  in Kelvin,  $t$  in seconds,  $k(\beta, T, t)$  from Eqn. (8) and  $\overline{c_{CS}(T)}$  from Eqn. (3).

The NOx level using Eqn. (9) are shown in Fig. 7 and 8.

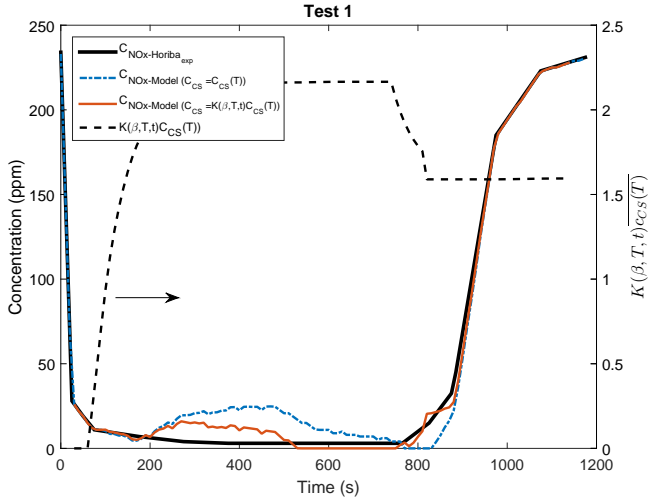


Fig. 7. Modeled NOx concentration - Maximum overshoot: 10 ppm, undershoot: 4 ppm (Eqn. (9), test1)

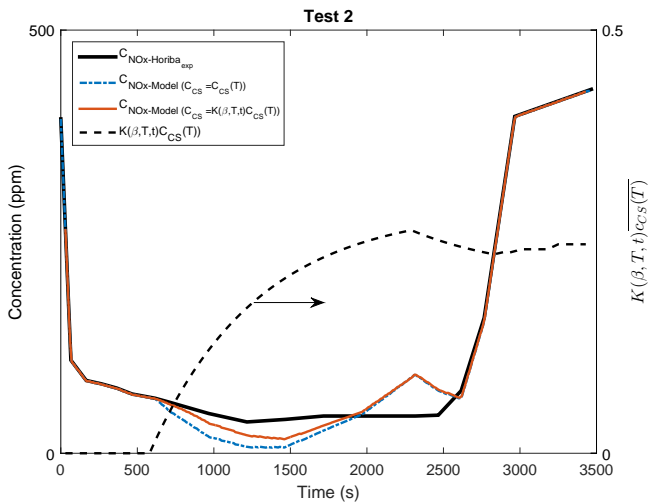


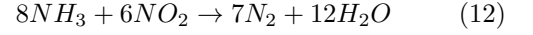
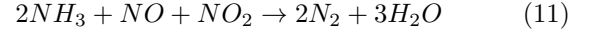
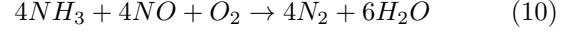
Fig. 8. Modeled NOx concentration - Maximum overshoot: 45 ppm, undershoot: 19 ppm (Eqn. (9), test2)

The model in Eqn. (9), follows the measured  $NO_x$  in Fig. 7 and 8 with a maximum overshoot (undershoot) of 10 (4) ppm and 45 (19) ppm instead of 34 (43) ppm and 48 (33) ppm for tests 1 and 2 respectively.

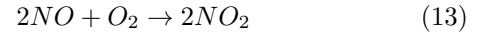
### 3. SELECTIVE CATALYST REDUCTION (SCR) MODEL

#### 3.1 Chemistry of the De-NOx SCR process

The main  $NO_x$  reduction reactions of SCR are described in Forzatti (2001) as:



NO is the dominant component of the engine-out  $NO_x$  emission and without using a Diesel Oxidation Catalyst (DOC), the NO concentration would be more than 90% of overall exhaust  $NO_x$  (Koebel et al., 2000). The reaction rate of Eqn. (10) is considered fast, so it is called the standard SCR reaction. Eqn. (11) is also called a fast SCR reaction, typically the fastest and the most preferred  $NO_x$  reduction reaction (Devarakonda et al., 2009). A DOC in the after-treatment system increases the amount of  $NO_2$  by the following reaction:



If the amount of  $NO_2$  is increased above a  $NO_2/NO$  ratio of one, then the undesirable slow reaction of Eqn. (12) takes place (Devarakonda et al., 2009).

#### 3.2 SCR reaction rates

The injected ammonia can be adsorbed on and desorbed from the SCR substrate. The kinetic rates of ammonia desorption and adsorption on the catalyst surface are calculated as Tronconi et al. (1996):

$$R_{des} = k_{des} \exp\left(\frac{E_{des}}{RT}\right) \theta_{NH_3} \quad (14)$$

$$R_{ads} = k_{ads} \exp\left(\frac{E_{ads}}{RT}\right) C_{NH_3} (1 - \theta_{NH_3}) \quad (15)$$

The reaction rate,  $R_{red}$ , of NOx reduction is defined by Hsieh and Wang (2010):

$$R_{red} = k_{red} \exp\left(\frac{E_{red}}{RT}\right) C_{NO_x} \theta_{NH_3} \quad (16)$$

where,  $R$  is ideal gas constant,  $T$  is the temperature and  $k_{red}$  and  $E_{red}$  are two constants.

Another main reaction that should be considered is the  $NH_3$  oxidation rate,  $R_{oxi}$ , which occurs at temperatures higher than 450 C and is represented as (Zhang et al., 2015):

$$R_{oxi} = k_{oxi} \exp\left(\frac{E_{oxi}}{RT}\right) \theta_{NH_3} \quad (17)$$

where  $k_{oxi}$  and  $E_{oxi}$  are two constants and  $\theta$  is the ammonia surface coverage ratio defined as:

$$\theta_{NH_3} = \frac{M_{NH_3}^*}{\Theta} \quad (18)$$

$M_{NH_3}^*$  is the mole of ammonia stored on the SCR substrate surface and  $\Theta$  is ammonia storage capacity (mole) described as (Sasaki et al., 2007):

$$\Theta = S_1 \exp(-S_2 T) \quad (19)$$

where  $S_1$  and  $S_2$  are constant.

### 3.3 SCR model formulation

A three-state nonlinear model was developed in Upadhyay (2006) using tailpipe  $NO_x$  and  $NH_3$  concentration and ammonia surface coverage ratio with the states:

$$\begin{bmatrix} \dot{C}_{NO_x} \\ \dot{\theta}_{NH_3} \\ \dot{C}_{NH_3} \end{bmatrix} = \begin{bmatrix} f_1(C_{NO_x}, \theta_{NH_3}, T, F) \\ f_2(C_{NO_x}, \theta_{NH_3}, T, C_{NH_3}) \\ f_3(C_{NH_3}, \theta_{NH_3}, T, F) \end{bmatrix} \quad (20)$$

$$+ \begin{bmatrix} 0 \\ 0 \\ F \end{bmatrix} C_{NH_3,up} + \begin{bmatrix} F \\ 0 \\ 0 \end{bmatrix} C_{NO_x,up}$$

where,

$$f_1(C_{NO_x}, \theta_{NH_3}, T, F) = -C_{NO_x}(\Theta r_{red}\theta_{NH_3} + \frac{F}{V}) + r_{oxi}\Theta\theta_{NH_3}$$

$$f_2(C_{NO_x}, \theta_{NH_3}, T, C_{NH_3}) = -\theta_{NH_3}(r_{red}C_{NH_3} + r_{des} + r_{red}C_{NO_x} + r_{oxi}) + r_{ads}C_{NH_3}$$

$$f_3(C_{NH_3}, \theta_{NH_3}, T, F) = -C_{NH_3}(\Theta r_{ads}(1 - \theta_{NH_3}) + \frac{F}{V}) + \Theta r_{des}\theta_{NH_3}$$

$C_{NO_x}$  and  $C_{NH_3}$  are tailpipe  $NO_x$  and  $NH_3$  concentrations, respectively,  $C_{NO_x,up}$  and  $C_{NH_3,up}$  are  $NO_x$  and  $NH_3$  concentrations upstream of the SCR, respectively,  $F[m^3/s]$  is the exhaust volume flow rate,  $V[m^3]$  is the catalyst volume,  $T[K]$  is exhaust gas temperature,  $\Theta$  is calculated from Eqn. (19) and  $r_{des}$ ,  $r_{ads}$ ,  $r_{red}$  and  $r_{oxi}$  are defined as:

$$r_i = \frac{R_i}{\theta}, \quad i = des, ads, red, oxi \quad (21)$$

### 3.4 Model Validation

To calibrate the parameters and validate the SCR model for different operating conditions, results from the literature (Hsieh and Wang, 2011) are used.

Simulated and experimental values of  $NH_3$  slip for test 1 are shown in Fig. 9. According to Fig. 9, the simulated  $NH_3$  slip (blue line) matches the measured values (yellow line) with maximum error of 21 ppm while the  $NH_3$  concentration upstream of the SCR is the red line from Hsieh and Wang (2011).

$NH_3$  slip is the output of the SCR model that is used in the next section.

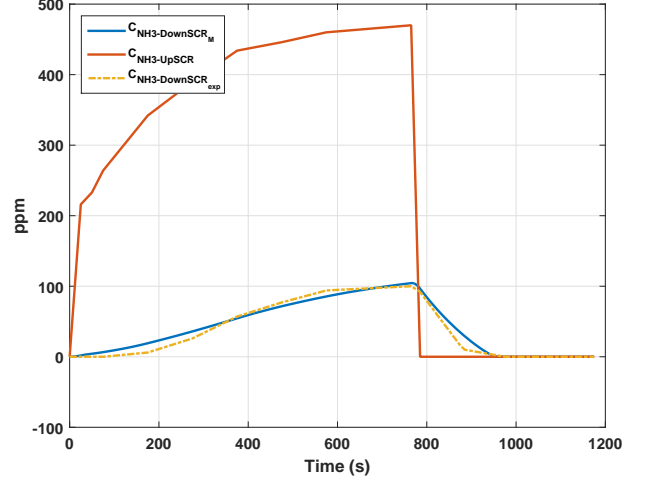


Fig. 9. Predicted  $NH_3$  concentration downstream of the SCR for test 1

## 4. COUPLING SCR AND $NO_x$ SENSOR MODEL

The SCR and  $NO_x$  sensor models are now coupled to estimate the actual  $NO_x$  concentration based on  $NO_x$  sensor signal and exhaust gas temperature upstream and downstream of SCR. A schematic of the coupled model is shown in Fig. 10.

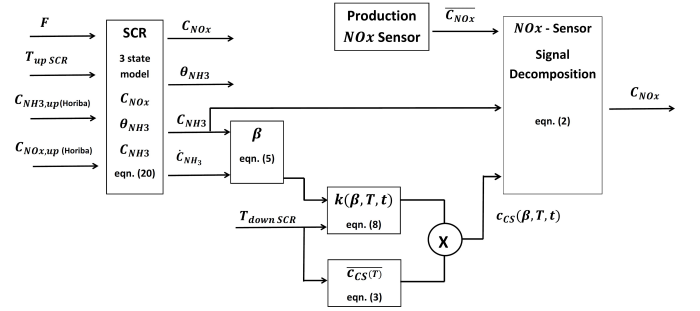


Fig. 10.  $NO_x$  concentration from coupled SCR and  $NO_x$  sensor model for test 1

Where,  $T_{up,SCR}[K]$  is the exhaust gas temperature upstream of SCR.

As indicated in Fig. 10,  $NH_3$  and  $NO_x$  concentration are both considered as inputs of the model. Although in this model  $NH_3$  and  $NO_x$  are measured by an accurate measurement device (Horiba MEXA 7500), it is not applicable for production engine management strategies. Therefore,  $NH_3$  and  $NO_x$  concentration should be measured or estimated. A simple practical method is using a production  $NO_x$  sensor upstream of the Adblue injector and modeling  $NH_3$  concentration based on the injected Adblue.

The simulated and experimental values of  $NH_3$  slip from the coupled SCR and  $NO_x$  sensor model are shown in Fig. 11 for test 1.

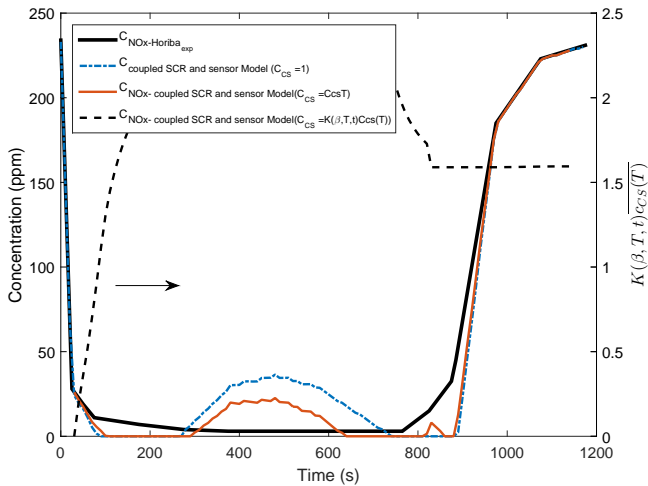


Fig. 11. NO<sub>x</sub> concentration from coupled SCR and NO<sub>x</sub> sensor model for test 1

The final C<sub>cs</sub> model (red line), Eqn. (9), has the closest value to the actual NO<sub>x</sub> concentration (black line) in comparison with all sensor models coupled to the SCR model as shown in Fig. 11. It should be noted that the error of all models consists of both sensor and SCR model errors.

## 5. CONCLUSIONS

Ammonia cross sensitivity of a production NO<sub>x</sub> sensor is modeled in this work for slow transients. The most effective factors on cross sensitivity were evaluated to get the best accuracy against the experiments. The model is validated for large amounts of ammonia slip. A dynamic production NO<sub>x</sub> sensor model is then developed to remove ammonia cross sensitivity and to decompose the NO<sub>x</sub> sensor output signal. A basic model is derived for the cross sensitivity factor based on the experiment data as a function of exhaust gas temperature. The model is then improved for transients by considering a correction factor as a function of normalized ammonia slip rate (NASR). A three-state nonlinear control oriented SCR model is also developed and used to predict the NH<sub>3</sub> concentration downstream of the SCR. The SCR model and the sensor model are finally coupled and NO<sub>x</sub> concentration is estimated using the NO<sub>x</sub> sensor signal decomposition. The validation results confirms that the model is capable to accurately estimate the actual NO<sub>x</sub> concentration based on the NH<sub>3</sub> concentration upstream of the SCR and the NO<sub>x</sub> sensor output signal. This model can be used for future engine emission control strategies such as SCR control.

## REFERENCES

Bonfils, A., Creff, Y., Lepreux, O., and Petit, N. (2014). Closed-loop control of a SCR system using a NO<sub>x</sub> sensor cross-sensitive to NH<sub>3</sub>. *Journal of Process Control*, 24(2), 368 – 378. ADCHEM 2012 Special Issue.

Devarakonda, M., Parker, G., Johnson, J., and Strots, V. (2009). Model-based control system design in a urea-SCR aftertreatment system based on NH<sub>3</sub> sensor feedback. *International Journal of Automotive Technology*, 10(6), 653–662.

Devarakonda, M., Parker, G., Johnson, J.H., Strots, V., and Santhanam, S. (2008). Model-based estimation and control system development in a Urea-SCR aftertreatment system. *SAE Int. J. Fuels Lubr.*, 1, 646–661.

Forzatti, P. (2001). Present status and perspectives in de-NO<sub>x</sub> SCR catalysis. *Applied Catalysis A: General*, 222(12), 221 – 236. Celebration Issue.

Frobert, A., Raux, S., Creff, Y., and Jeudy, E. (2013). About cross-sensitivities of NO<sub>x</sub> sensors in SCR operation. SAE 2013-01-1512.

Hsieh, M.F. and Wang, J. (2010). An extended Kalman filter for NO<sub>x</sub> sensor ammonia cross-sensitivity elimination in selective catalytic reduction applications. In *American Control Conference (ACC), 2010*, 3033–3038.

Hsieh, M.F. and Wang, J. (2011). Development and experimental studies of a control-oriented SCR model for a two-catalyst urea-SCR system. *Control Engineering Practice*, 19(4), 409 – 422.

Jones, J.C.P. and Geveci, M. (2011). Smart sensing and decomposition of NO<sub>x</sub> and NH<sub>3</sub> components from production nox sensor signals. *SAE Int. J. Engines*, 4, 1393–1401.

Koebel, M., Elsener, M., and Kleemann, M. (2000). Urea-SCR: a promising technique to reduce NO<sub>x</sub> emissions from automotive Diesel engines. *Catalysis Today*, 59(34), 335 – 345.

Sasaki, S., Sarlashkar, J., Neely, G.D., Wang, J., Lu, Q., and Sono, H. (2007). Investigation of alternative combustion, airflow-dominant control and aftertreatment system for clean Diesel vehicles. SAE 2007-01-1937.

Schar, C., Onder, C., and Geering, H. (2006). Control of an SCR catalytic converter system for a mobile heavy-duty application. *IEEE Transactions on Control Systems Technology*, 14(4), 641–653.

Tronconi, E., Lietti, L., Forzatti, P., and Malloggi, S. (1996). Experimental and theoretical investigation of the dynamics of the SCR - denox reaction. *Chemical Engineering Science*, 51(11), 2965 – 2970. *Chemical Reaction Engineering: From Fundamentals to Commercial Plants and Products*.

Upadhyay, Devesh Van Nieuwstadt, M. (2006). Model based analysis and control design of a Urea-SCR deNO<sub>x</sub> aftertreatment system. *Journal of Dynamic Systems, Measurement, and Control*, 128, 737–741.

Willems, F., Cloudt, R., van den Eijnden, E., van Genderen, M., Verbeek, R., de Jager, B., Boomsma, W., and van den Heuvel, I. (2007). Is closed-loop SCR control required to meet future emission targets? SAE 2007-01-1574.

Zhang, H. and Wang, J. (2015). Ammonia coverage ratio and input simultaneous estimation in ground vehicle selective catalytic reduction (SCR) systems. *Journal of the Franklin Institute*, 352(2), 708 – 723. Special Issue on Control and Estimation of Electrified vehicles.

Zhang, H., Wang, J., and Wang, Y.Y. (2015). Removal of sensor ammonia cross sensitivity from contaminated measurements in Diesel-engine selective catalytic reduction systems. *Fuel*, 150(0), 448 – 456.